THz and SHG autocorrelation generations in reflection from different nonlinear crystals excited by femtosecond laser pulses

Kristensen, Mathias Hedegaard; Skovsen, Esben; Herault, Emilie; Coutaz, Jean-Louis

Published in:
2024 49th International Conference on Infrared, Millimeter, and Terahertz Waves (IRMMW-THz)

DOI (link to publication from Publisher):
10.1109/IRMMW-THz60956.2024.10697733

Publication date:
2024

Document Version
Early version, also known as pre-print

THz and SHG autocorrelation generations in reflection from different nonlinear crystals excited by femtosecond laser pulses

Mathias H. Kristensen and Esben Skovsen
Dept. of Materials and Production
Aalborg University
Aalborg, Denmark
mhkr@icloud.com, es@mp.aau.dk

Emilie Hérault and Jean-Louis Coutaz
CROMA
University Savoie Mont Blanc
Le Bourget du Lac, France
emilie.herault@univ-smb.fr, coutaz@univ-smb.fr

***Abstract*—We present an autocorrelation technique for very-broadband characterization of weak terahertz and second-harmonic beams generated in reflection by surface excitation of nonlinear crystals by femtosecond laser pulses.**

***Index Terms*—terahertz waves, optical rectification, second-harmonic generation, femtosecond pulses, autocorrelation.**

I. Introduction

Exciting a nonlinear (NL) crystal by two successive femtosecond laser pulses and varying the time delay τ between the two pulses permits to perform an autocorrelation study of second-order nonlinear processes, like THz generation by optical rectification (OR) or second-harmonic generation (SHG). As compared to classical single-shot experiments, this technique allows one to use very sensitive energy detectors, like cryogenic bolometers or photomultiplier tubes (PMT), and delivers very broadband spectra, whose upper frequency value is only limited by the bandwidth of the detectors. We already demonstrated this technique [1] for THz and SHG generations by reflection at the surface of a ZnTe crystal: In this case, the autocorrelation technique is useful because the reflected signals are weak. We have shown that both THz and SHG spectra show a low-frequency (THz) part, which resembles the spectra achieved with classical single pulse spectroscopy using ultrafast detectors, as well as spectral features centered respectively around the laser optical frequency ω_o (namely $f_o = \omega_o/2\pi = 375$ THz) and its second-harmonic at $2f_o = 750$ THz.

Here we present a similar and complementary study performed with GaSe, $LiNbO_3$, and GaP crystals. These new results clearly evidence that the NL generation occurs at the surface of the crystals, and thus, is not perturbed by phase-matching effects or absorption in the crystals. Moreover, the so-recorded THz spectra exhibit specific features related to each crystal, like dips resulting from the excitation of phonons.

II. Analysis of Modeling Results

Let us give here a summary of the main modeling results published in Ref. [1]. In a plane wave calculation, the amplitude of the reflected NL field, either at THz frequencies through OR, or at SH frequencies, writes:

$$E_{\mathrm{r}}(\omega) = -\frac{c^2 \mu_o P^{(2)}(\omega)}{\left(\tilde{n}_\omega + \tilde{N}\right)\left(\tilde{n}_\omega + 1\right)}. \tag{1}$$

ω is the angular frequency, c is the speed of light in vacuum, μ_o is the permeability of vacuum, $\tilde{n}_\omega$ is the complex refractive index of the crystal at frequency ω, $P^{(2)}(\omega)$ is the nonlinear polarization at the crystal surface. When dealing with THz OR, $\tilde{N}$ is the group index $\tilde{n}_G(\omega_o)$ at the laser frequency while it is the refractive index $\tilde{n}(\omega_o)$ when dealing with SHG. It does not depend on propagation in the crystal, and thus the reflected beam should not exhibit phase-matching effect. On the other hand, it depends slightly on the absorption at both the laser frequency and the NL frequency through the denominator. Finally, the dispersion of the nonlinearity is underlying in $P^{(2)}(\omega)$. In the case of a double laser pulse excitation, the expressions are more complicated. We can simplify them for Gaussian-shaped laser pulses (i.e. $f(t) \propto \exp[-(t/\tau_{\mathrm{las}})^2]$) if we neglect the dispersion of the nonlinearity. Thus we get the spectra of the waveforms recorded versus τ for both THz OR and second-harmonic (SH) signals:

$$\begin{aligned} S_{\mathrm{THz}}(\omega) \propto\ & \exp\!\left[-\tfrac{\omega^2\tau_{\mathrm{las}}^2}{4}\right] \\ & + \tfrac{2}{\sqrt{3}}\exp\!\left[-\tfrac{(\omega-\omega_o)^2\tau_{\mathrm{las}}^2}{3}\right] \\ & + \tfrac{1}{4}\exp\!\left[-\tfrac{(\omega-2\omega_o)^2\tau_{\mathrm{las}}^2}{4}\right], \end{aligned} \tag{2}$$

$$\begin{aligned} S_{\mathrm{SH}}(\omega) \propto\ & \exp\!\left[-\tfrac{\omega^2\tau_{\mathrm{las}}^2}{4}\right] \\ & + \tfrac{4}{\sqrt{3}}\left(1+\mathrm{erf}\!\left[\tfrac{(\omega-\omega_o)\tau_{\mathrm{las}}}{\sqrt{6}}\right]\right)\exp\!\left[-\tfrac{(\omega-\omega_o)^2\tau_{\mathrm{las}}^2}{3}\right] \\ & + \tfrac{1}{2}\exp\!\left[-\tfrac{(\omega-2\omega_o)^2\tau_{\mathrm{las}}^2}{4}\right]. \end{aligned} \tag{3}$$

The first term on the right side of Eq. (2) and Eq. (3) is the THz part of the spectra, the second one is centered around ω_o and is called the optical term, while the last one is the SH term centered at $2\omega_o$.

III. Experimental Results

The GaSe, $LiNbO_3$, and GaP crystals were pumped by two successive laser pulses delivered by a Michelson interferometer that was fed by an amplified Ti:sapphire laser system (Spectra-Physics Spitfire, $\lambda = 800$ nm, 1-kHz rep. rate). At the sample, the maximum peak power density was 75 GW/cm^2. The laser beam impinged the sample at normal incidence through a hole in a parabolic mirror. This mirror collected the reflected THz radiation and directed it towards a Schottky diode THz receiver (in front of it, a THz low-pass filter blocked the residual laser light). Because the reflected generated SH beam was almost parallel, it went back through the hole and a dichroic filter reflected it towards a PMT. Getting the THz part of the spectra required measurements over a long time-window with a rather longer step (2 fs - translation stage with a stepper motor), while the optical and SH spectral features required a shorter temporal step (0.02 fs - piezo stepping drive).

IV. Results and Discussion

Fig. 1 presents the THz spectra delivered by GaP samples of 200- and 300-μm thicknesses. The two curves are almost

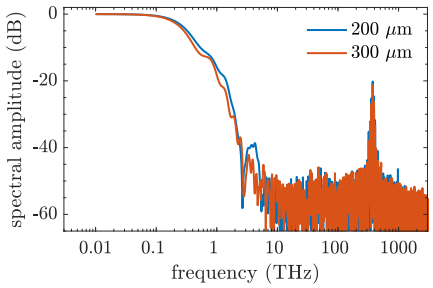

Fig. 1. autocorrelation spectra of the THz signal delivered by GaP crystals of thicknesses 200-μm (blue curve) and 300-μm (red curve).

identical, demonstrating as expected that THz generation in reflection does not depend on the sample thickness (Let us notice that the same curves but recorded in transmission would have differed at least by a factor of 2.25, i.e. 3.55 dB). Moreover, the region at the crystal surface that radiates the NL reflected beams is thinner than 200-μm. This is true even at the smaller frequencies of the recorded spectra ($\sim$50 GHz, i.e. $\lambda = 6$ mm). Therefore, the hypothesis of a "formation length", whose thickness is of the order of the THz wavelength [3], is controversial. The optical peak at 375 THz is clearly seen. The shape and upper limit (-50 dB at 3 THz) of the THz part of the curves is due to the spectral responsivity of the Schottky diode receiver. The THz and SH spectra supplied by the $LiNbO_3$ sample are plotted in Fig. 2. $LiNbO_3$ exhibits a strong phase-mismatch due to the large difference between its optical and THz indices [2]. However, the sinc-function shape due to phase-mismatch is not seen here which proves that both THz and SH reflected signals are not sensitive to propagation effects inside the crystal. The narrower THz part of the THz spectrum is due to the huge absorption of $LiNbO_3$ over 1 THz [2], while the SH spectrum is almost similar to the

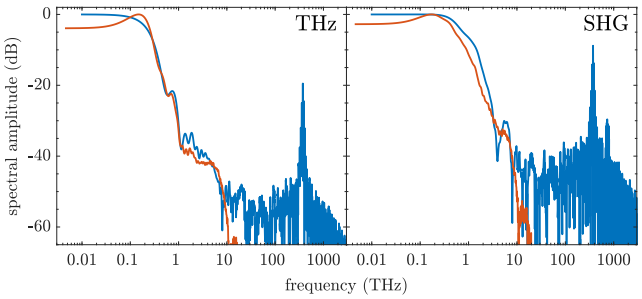

Fig. 2. autocorrelation spectra of the THz (left) and SH (right) signals delivered by a 1-mm thick $LiNbO_3$ crystal; blue curve: high temporal resolution spectrum, red curve: waveform envelop spectrum.

THz GaP one (Fig. 1) and slightly broader thanks to the larger bandwidth of the PMT. Here the SH peak at 750 THz is also seen. The noise level originates mostly from the laser pulse-to-pulse variation and also from the receiver sensitivity. Finally,

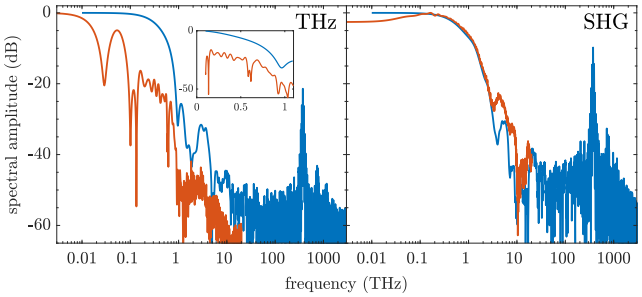

Fig. 3. autocorrelation spectra of the THz (left) and SH (right) signals delivered by a 1-mm thick GaSe crystal.

Fig. 3 depicts the THz and SH spectra from a 1-mm thick GaSe crystal. The well-known phonon absorption line at 600 GHz is clearly observed in the THz spectrum, demonstrating that the autocorrelation technique delivers information on the THz response of the crystal. On the other hand, this phonon line does not appear in the SHG spectrum. Therefore, the lattice deformation induced by the phonon is not large enough to modify the SH nonlinear susceptibility.

In conclusion, we have demonstrated in this study that autocorrelation THz and SH generations in reflection is a high-performance technique that allows one characterizing THz and SH emission from nonlinear crystals over a very large bandwidth even if the signals are weak.

References

[1] M. Kristensen, E. Skovsen, E. Hérault and J.-L. Coutaz, "Autocorrelation study of terahertz and second-harmonic pulsed generations in reflection at the surface of a nonlinear dielectric crystal," submitted to Optics and Laser Technology (2024).

[2] X. Wu, C. Zhou, W. R. Huang, F. Ahr, and F. X. Kärtner, "Temperature dependent refractive index and absorption coefficient of congruent lithium niobate crystals in the terahertz range," Optics Express **23**, 29729 (2015).

[3] N. N. Zinov'ev, A. S. Nikoghosyan, J. M. Chamberlain, "Conversion of short optical pulses to terahertz radiation in a nonlinear medium: Experiment and theory," Phys. Rev. **B 76**, 235114 (2007).